Resolution of the fluorescence equilibrium unfolding profile of Trp apo-repressor using single tryptophan mutants

ARTICLE *in* PROTEIN SCIENCE · NOVEMBER 1993

Impact Factor: 2.85 · DOI: 10.1002/pro.5560021106 · Source: PubMed

3 AUTHORS, INCLUDING:

Catherine A Royer
Rensselaer Polytechnic Institute
172 PUBLICATIONS **5,532** CITATIONS
SEE PROFILE

Charles Robert Matthews
University of Massachusetts Medical School
146 PUBLICATIONS **5,900** CITATIONS
SEE PROFILE

Protein Science (1993), *2*, 1844-1852. Cambridge University Press. Printed in the USA.

Resolution of the fluorescence equilibrium unfolding profile of *trp* aporepressor using single tryptophan mutants

CATHERINE A. ROYER,[1] CRAIG J. MANN,[2,3] AND C. ROBERT MATTHEWS[2]

[1] School of Pharmacy, University of Wisconsin at Madison, Madison, Wisconsin 53706
[2] Department of Chemistry, The Center for Biomolecular Structure and Function, and The Biotechnology Institute, The Pennsylvania State University, University Park, Pennsylvania 16802

(RECEIVED April 2, 1993; ACCEPTED August 9, 1993)

Abstract

Single tryptophan mutants of the *trp* aporepressor, tryptophan 19 → phenylalanine (W19F) and tryptophan 99 → phenylalanine (W99F), were used in this study to resolve the individual steady-state and time-resolved fluorescence urea unfolding profiles of the two tryptophan residues in this highly intertwined, dimeric protein. The wild-type protein exhibits a large increase in fluorescence intensity and lifetime, as well as a large red shift in the steady-state fluorescence emission spectrum, upon unfolding by urea (Lane, A.N. & Jardetsky, O., 1987, *Eur. J. Biochem. 164*, 389-396; Gittelman, M.S. & Matthews, C.R., 1990, *Biochemistry 29*, 7011-7020; Fernando, T. & Royer, C.A., 1992, *Biochemistry 31*, 6683-6691). Unfolding of the W19F mutant demonstrated that Trp 99 undergoes a large increase in intensity and a red shift upon exposure to solvent. Lifetime studies revealed that the contribution of the dominant 0.5-ns component of this tryptophan tends toward zero with increasing urea, whereas the longer lifetime components increase in importance. This lifting of the quenching of Trp 99 may be due to disruption of the interaction between the two subunits upon denaturation, which abolishes the interaction of Trp 99 on one subunit with the amide quenching group of Asn 32 on the other subunit (Royer, C.A., 1992, *Biophys. J. 63*, 741-750). On the other hand, Trp 19 is quenched in response to unfolding in the W99F mutant. Exposure to solvent of Trp 19, which is buried at the hydrophobic dimer interface in the native protein, results in a large red shift of the average steady-state emission. Thus, changes in the fluorescence properties of the two intrinsic tryptophan residues in *trp* aporepressor upon unfolding are explained readily in terms of disruption of the dimer interface.

Keywords: mutagenesis; protein folding; *trp* aporepressor; tryptophan fluorescence

Fluorescence spectroscopy offers a variety of static and dynamic properties that are useful for monitoring protein-unfolding reactions induced by heat, chemical denaturants, or pressure. This application relies on the sensitivity of intrinsic tryptophan and tyrosine residues to their immediate environment. Changes in local environment generally coincide with the global loss of secondary and tertiary structure because the unfolding transitions of many proteins are highly cooperative. Thus, the dependence of steady-state fluorescence intensity or emission energy on the concentration of the denaturant can provide values for the free energy of folding (Tanford, 1970; Pace, 1986).

Although such applications of fluorescence spectroscopy are employed widely, difficulties inherent in resolving the contributions of individual chromophores in multichromophore-containing proteins (Beechem & Brand, 1985; Harris & Hudson, 1990; Royer et al., 1990; Axelson et al., 1991; Royer, 1992) limit interpretations of the structural and dynamic properties of these side chains during unfolding. A potential solution to this problem is to replace fluorescent side chains, e.g., tryptophan, with a nonfluorescent aromatic side chain, e.g., phenylalanine, using site-directed mutagenesis followed by examination of the remaining fluorophore(s). For the case in which a single fluorescent side chain remains, studies of its total fluorescence intensity, average emission intensity, bandwidth of emission spectrum, and evolution of lifetime compo-

Reprint requests to: Catherine A. Royer, School of Pharmacy, University of Wisconsin at Madison, Madison, Wisconsin 53706.
[3] Present address: Eli Lilly and Company, Lilly Corporate Center Mail Drop Code 3227, Indianapolis, Indiana 46285.

Abbreviations: DAS, decay-associated spectra; NATA, *n*-acetyltryptophanamide; TR, *trp* aporepressor; W19F, tryptophan 19 → phenylalanine; W99F, tryptophan 99 → phenylalanine.

nents at varying denaturant concentrations could provide a detailed view of its local environment during the unfolding process. For proteins containing more than two fluorophores, comparison of the results for the single mutant with the wild-type protein could reveal, in favorable cases, properties of the residue being replaced.

The tryptophan aporepressor (TR) from *Escherichia coli* provides an interesting test of this hypothesis. The TR is a small protein, 12.6 kDa per monomer, which contains two intrinsic tryptophan residues per monomeric subunit. Although it has been crystallized as a dimer (Zhang et al., 1987), it has been shown in solution in the range of 0.1 to 100 μM to be in equilibrium between dimers and higher order oligomers (Fernando & Royer, 1992a). Equilibrium unfolding studies of TR, which observed both the intrinsic fluorescence and that of extrinsic probes (Gittelman & Matthews, 1990; Fernando & Royer, 1992b), demonstrated that dissociation of the tetramers occurred at urea concentrations much lower than the concerted dimer dissociation–unfolding transition. In addition, Fernando and Royer (1992b) have confirmed that the intrinsic tryptophan fluorescence is almost completely insensitive to the tetramer–dimer transition, and report only on dimer unfolding.

The structure of the TR dimer, deduced from X-ray crystallographic data, shows that each subunit contains six α-helices (Fig. 1; Kinemage 1). The core consists of an interface in which the A, B, and C helices from each subunit are interlocked. The D and E helices are arranged in a helix–turn–helix motif, and comprise the DNA-binding domain of the protein. The F helices complete the core. The two tryptophan residues, Trp 19 in helix A and Trp 99 in helix F, are pictured in Figure 1. The emission properties of these two tryptophan residues in the native protein have been resolved using single tryptophan mutants (Royer, 1992). Trp 19, which is buried at the subunit interface in an extremely hydrophobic environment, exhibits a very blue-shifted emission, with an average lifetime between 3 and 4 ns. Trp 99 in the F helix and docked on the core has a much redder emission spectrum, reflecting its polar environment and exposure to solvent. An asparagine residue from the opposite subunit, Asn 32, has been proposed as the quenching group that leads to the dominance of emission by a 0.5-ns component (Royer, 1992).

The wild-type TR exhibits a large increase in intensity and a red shift in emission upon unfolding by urea (Lane & Jardetsky, 1987; Gittelman & Matthews, 1990; Fernando & Royer, 1992b). Lane and Jardetsky (1987) were able to partially resolve contributions from the two tryptophan residues to the denaturation profile by observing intensity changes on the red and blue edges of the spectrum. Given the structure of TR and the resolution of fluorescence decay properties of intrinsic tryptophan residues in the native state, it was proposed that lifting of the quenching of Trp 99 was responsible for the increased intensity observed upon unfolding of the wild-type protein (Royer, 1992).

This paper describes steady-state and time-resolved fluorescence parameters as a function of urea concentration for two single tryptophan mutants: tryptophan 19 → phenylalanine (W19F) and tryptophan 99 → phenylalanine (W99F). These studies allow unambiguous assignment of

Fig. 1. Ribbon diagram of dimeric *trp* aporepressor taken from the structure of Zhang et al. (1987). The individual subunits are indicated in blue and magenta, respectively. The side chains of the two tryptophan residues, 19 (indicated in yellow) and 99 (indicated in green), are also shown.

fluorescence changes in the wild-type protein to the individual tryptophan residues. In turn, the results lead to conclusions about structural changes responsible for fluorescence perturbations.

Results

Steady-state fluorescence unfolding profiles

The steady-state fluorescence emission spectra of W99F and W19F were measured as a function of urea concentration between 0 and 9 M urea (Fig. 2). The emission of Trp 19 in W99F at 0 M urea is, as determined previously (Royer, 1992), quite blue shifted, with a maximum near 319 nm (Fig. 2A). The spectrum shifts significantly to longer wavelengths, and there is an overall decrease in the fluorescence intensity as urea concentration increases (Fig. 2A). The effect of urea on Trp 99 in W19F is quite different (Fig. 2B). The spectrum in the native state is redder than that of Trp 19, and the quantum yield is much lower (Royer, 1992). In contrast to W99F, a large *increase* in intensity and a significant red shift is observed when W19F is unfolded by urea. The red shift in emission for these proteins was determined by calculating the intensity-averaged emission wavelength, $\langle\lambda\rangle$, using the equation

$$\langle\lambda\rangle = \sum_{i=1}^{N} (I_i\lambda_i) \Big/ \sum_{i=1}^{N} (I_i). \qquad (1)$$

This quantity is less prone to instrumental noise than is the peak maximum because it is an integral measurement. It is also a more sensitive value because it arises from a calculation involving the entire spectrum, and thus it reflects changes in the shape of the spectrum as well as in position. The smaller red shift in the average emission wavelength for W19F, 12 nm, versus the 22-nm shift found for W99F reflects the bluer emission of Trp 19 in the native state. At 9 M urea, the steady-state emission spectra of the two tryptophan residues are nearly identical, as would be expected for fully solvated residues.

Preliminary fit of fluorescence data from the single tryptophan mutants to a two-state model (Fig. 2, insets) (Gittelman & Matthews, 1990; Fernando & Royer, 1992b) yield apparent free energies of folding in the absence of denaturant of 18.4 ± 1.1 and 20.7 ± 0.8 kcal/mol (dimer), respectively, for W19F and W99F. The average emission wavelength data were fit by a model in which quantum yield differences between the native and denatured states were taken into account. These values are in the same range as that obtained for the wild-type protein, 18.2 kcal/mol, using the same method (see Fig. 1 in the accompanying paper by Mann et al. [1993]).

The evolution of the total intensity of the emission spectrum of Trp 19, i.e., in W99F as a function of urea, is shown in Figure 3A; Figure 3B–D displays the intensities measured at 320, 350, and 380 nm, respectively. The intensity profile observed depends upon the wavelength at which the observation is made because the emission wavelength shifts with unfolding. The intensity at 320 nm decreases in a sigmoidal fashion between 2 and 6 M urea; the native and unfolded baselines are almost independent of denaturant concentration. Although the intensity at

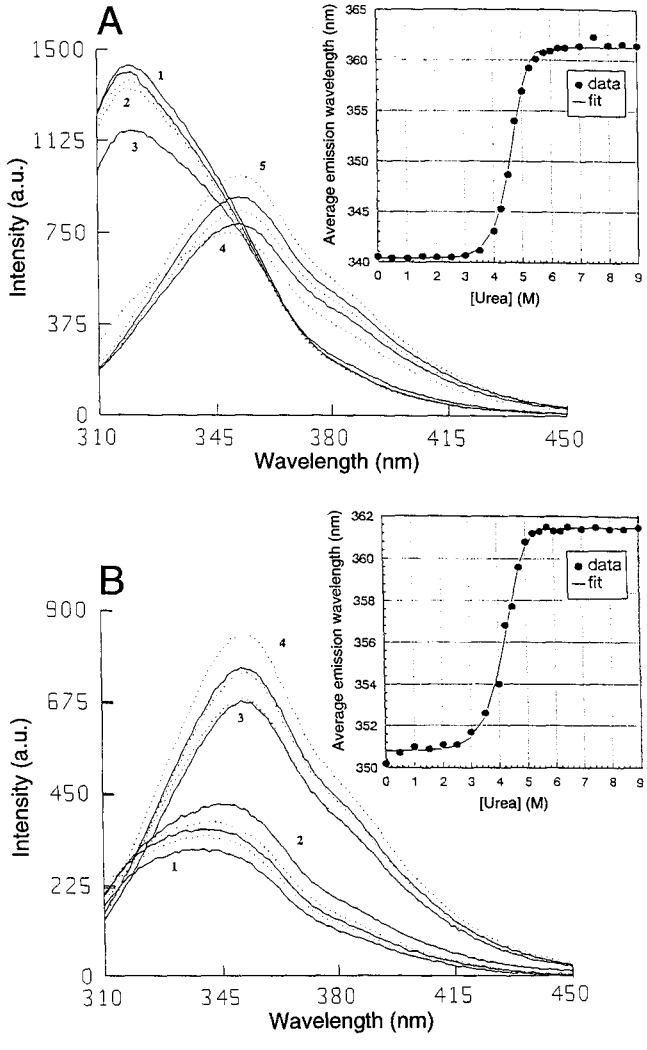

Fig. 2. Evolution of the intrinsic tryptophan emission spectrum as a function of urea concentration between 0 and 9 M urea. Insets represent the average emission wavelength calculated from the spectra and fit to a two-state denaturation transition. **A:** W99F mutant, 5.5 μM in dimer; spectra are 0–9 M urea in 1 M urea steps alternating solid and dashed lines; numbered spectra correspond to (1) 0 M urea, (2) 3 M urea, (3) 4 M urea, (4) 5 M urea, and (5) 9 M urea. Between 5 and 9 M urea, the intensities increase. The total intensities corresponding to the peak integrals of these spectra are plotted in Figure 3A. **B:** W19F mutant, 6.1 μM in dimer; spectra are 0–9 M urea in 1 M urea steps alternating solid and dashed lines; numbered spectra correspond to (1) 0 M urea, (2) 4 M urea, (3) 5 M urea, and (4) 9 M urea. Between 5 and 9 M urea, the intensities increase. The total intensities corresponding to the peak integrals of these spectra are plotted in Figure 4A. Excitation was at 295 nm.

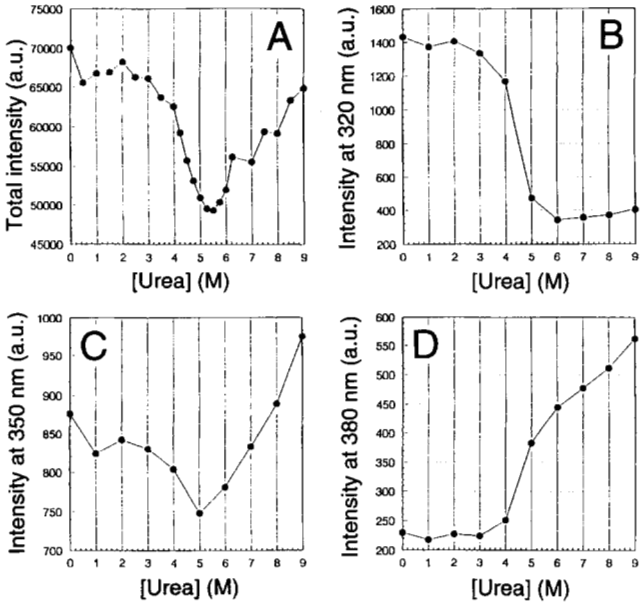

Fig. 3. Evolution of the fluorescence intensity of W99F as a function of urea concentration. **A:** Total intensity of the spectra in Figure 2A. **B:** Intensity observed at 320 nm. **C:** Intensity observed at 350 nm. **D:** Intensity observed at 380 nm. Excitation was at 295 nm. Data were taken from the experiments in Figure 2A.

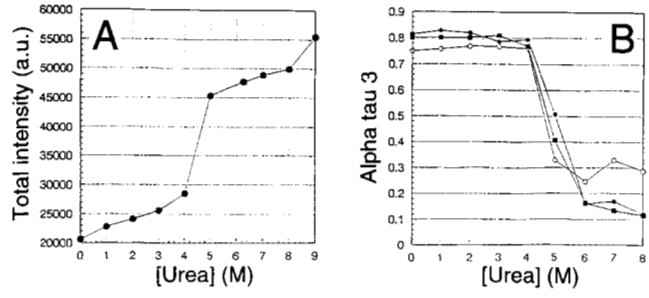

Fig. 4. A: Evolution of the total intensity of the intrinsic emission of W19F as a function of urea concentration taken from the spectra in Figure 2B. **B:** Evolution of the molecular fraction emitting with the 0.57-ns lifetime as a function of urea concentration at 320 nm (○), 350 nm (●), and 380 nm (■) emission. Protein concentration was 5.5 μM in dimer.

380 nm also increases between 2 and 6 M urea, it continues to increase above 6 M urea. The behavior of the intensity at 350 nm is similar to the total, exhibiting a decrease in intensity from 2 to 5 M urea, followed by an increase above 5 M urea. The dependence above 5 M urea is likely to reflect the presence of urea in the solvent. The same effect is observed on the intensity of NATA, which varies approximately 4% per mole/liter of urea (data not shown). Comparing the intensity values in Figure 3 with the spectra in Figure 2A, one can see that between 0.5 and 2 M urea, the emission energy of Trp 19 does not change, yet the intensity increases slightly. This is followed by a red shift between 3.5 and 6 M urea and a loss in overall intensity.

The change in total intensity of Trp 99 in W19F, plotted in Figure 4A, shows a gradual increase up to 4 M urea, followed by an abrupt increase between 4 and 5 M urea. The intensity then continues to increase in a monotonic fashion above 5 M urea, similar to the behavior for W99F (Fig. 2A).

Time-resolved fluorescence

The frequency response of the intrinsic fluorescence of W19F and W99F was measured as a function of both emission wavelength and urea concentration. It has been shown that urea unfolding results in a loss of a 0.5-ns component in the wild-type protein and an increase in width and center value of the distribution, which best describes the remaining decay components (Fernando & Royer, 1992b). The frequency response profiles for W99F at 320, 350, and 380 nm as a function of urea concentration are given in Figure 5A–C. The profiles at 320 nm shift to higher frequency as a function of urea, with a sharp transition between 4 and 6 M corresponding to the decrease in fluorescence intensity during the main transition. At 350 nm, the profiles shift to higher frequency (shorter lifetime) until 6 M urea, and then at 8 M urea, shift slightly toward lower frequency. At 380 nm, this reversal of the quenching trend is even more evident, with the highest frequency response at 4 M urea, followed by a shift to a lower frequency at 6 and 8 M urea.

These data sets were fit individually in terms of distributions of single-, double-, and triple-exponential decays to determine the number and dependence of lifetimes on denaturant concentration. In addition, lifetime values were linked across wavelength data sets for individual urea concentrations and across urea concentration data sets for individual wavelengths. The results of this approach will not be presented here. Overall, the urea-induced shifts in frequency response curves in Figure 5 were very small. The major component with values ranging between 3.5 and 4.5 ns was evident in every analysis, linked or unlinked, distributed or discrete, for all wavelengths and urea concentrations. In order to account for the small shifts toward higher frequencies with increasing urea, a shorter component near 0.3–1.0 ns was needed. The distributions shifted slightly to lower average lifetime and broadened considerably. What was clear from these fits was that the recovered lifetime values were quite similar, regardless of the linkage scheme, whereas the pre-exponential factors varied with wavelength and urea.

A fit was then attempted in which lifetimes in a triple-exponential decay scheme were linked across all 27 data sets for each mutant, all wavelengths, and all urea concentrations, with the pre-exponential factors unlinked. This linkage scheme gave a surprisingly satisfactory fit

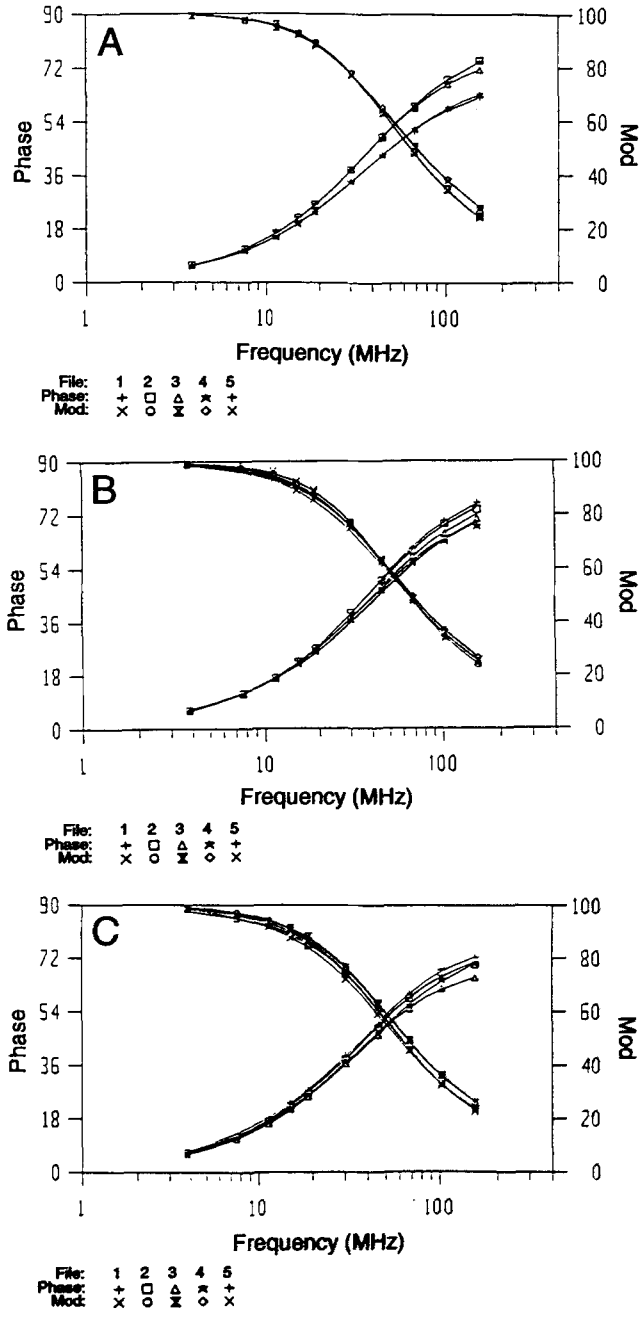

Fig. 5. Frequency response profiles of the intrinsic fluorescence of W99F at 0, 2, 4, 6, and 8 M urea. Mod and Phase indicate the modulation ratio and phase angle, respectively. Symbols numbered 1-5 correspond to the phase angles and modulation ratios for the five urea concentrations (0, 2, 4, 6, and 8 M). A: A 320-nm emission wavelength. B: A 350-nm emission wavelength. C: A 380-nm emission wavelength. Excitation was at 295 nm and the protein concentration was 5.5 μM in dimer.

(global χ^2 of 3.4) for the W99F mutant. Only three data sets, those at 380 nm for 1, 2, and 3 M urea, were not compatible with the scheme. Their local χ^2 values were between 10 and 20. However, all other data sets were quite consistent with this picture. For comparison, the χ^2 for individual data sets for single distributions unlinked across urea at 350 nm varied from 2.5 at 0 M urea to 8.7 at 8 M urea. The χ^2 values for the unlinked analysis at 380 nm for a triple-exponential decay ranged from 1.01 to 4.75. Thus, there is no significant χ^2 penalty for linking lifetime values across all 27 data sets. The χ^2 values in the frequency domain analysis do not denote an absolute goodness of fit. Rather, they can be used to compare the goodness of fit for different decay models to the same data surface. Therefore, the goodness of fit for the model in which lifetimes were linked across both wavelength and urea concentration was comparable to the χ^2 values in unlinked analyses. The values for the three recovered lifetimes were 20, 4.3, and 0.73 ns, respectively, for components 1, 2, and 3. In the absence of urea, the analysis yielded almost none of the longer component. This result resembles the slightly heterogeneous decay of Trp 19 in the native state of W99F (between 3 and 4 ns) observed previously using five rather than three emission wavelengths (Royer, 1992).

The DAS for W99F are plotted as a function of urea in Figure 6. The 20-ns component is not shown because its contribution was less than 2% of the population and less than 9% of the intensity. In fact, its value in the unlinked analyses ranged from 4.5 to 27 ns, with compensating fluctuations in its pre-exponential term. Given that this long component contributes very little to the signal, the actual value of the lifetime is not uniquely recovered from the fit, but simply reflects a long lifetime heterogeneity in the emission. The profile of its fractional molecular population (alpha tau 1) at three wavelengths as a function of urea is presented in Figure 7A. Although the predicted populations are scattered, at 380 nm they somewhat resemble the total intensity profile (Fig. 3A). The spectrum of the dominant component in the absence of urea (4.25 ns lifetime; Fig. 6) shifts to the red, and its total molecular fraction (alpha tau 2), decreases at all wavelengths upon unfolding (Fig. 7B). The slight increase in lifetime between 0 and 4 M urea is apparently due to an increased population of the component. The contribution of the shortest lifetime (0.75 ns) increased with increasing urea concentration (Fig. 7c). The contributions, or alpha values, reported in Figure 7 are in terms of the pre-exponential factor or molecular concentration for each species, whereas the DAS in Figure 6 are weighted for fractional intensity values. The loss of total intensity during the main unfolding transition is thus due at least partially to a decrease in contribution from the 4.3-ns component and an increase in that from the 0.75-ns component. However, although the data in Figure 7 demonstrate a general decrease in the 4.3-ns component at all wavelengths upon increasing urea, as well as increase in the 0.75-ns component, the total intensity profiles in Figure 3 show a loss of intensity in the blue and a gain in the red. In fact, this is not inconsistent because a good proportion of the intensity gain in the red is due to a shift in

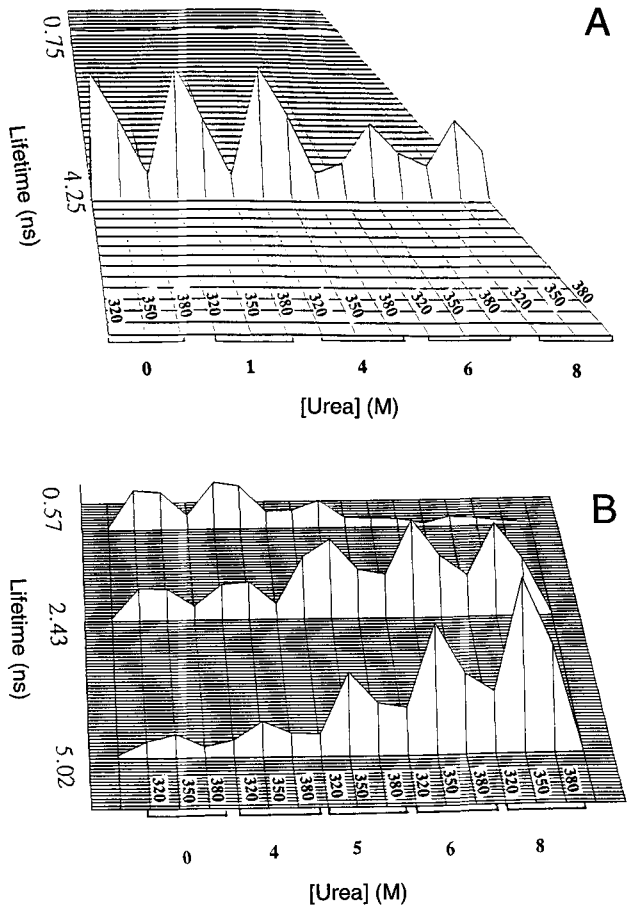

Fig. 6. Decay-associated spectra (DAS) as a function of urea concentration for (**A**) W99F at 0, 1, 4, 6, and 8 M urea, and (**B**) W19F at 0, 4, 5, 6, 7, and 8 M urea. Three emission wavelengths are plotted for each urea concentration (320, 350, and 380 nm). These DAS result from a global analysis of 27 data sets in which lifetimes were linked across all wavelengths and urea concentrations and the fractional contributions to the intensity were allowed to vary between data sets. Global χ^2 was 3.9. The longest lifetime component for W99F is not pictured in A so that the other, more significant DAS may be visualized more easily.

the emission spectrum, not to a change in fluorescence lifetime. Nonetheless, modifications in static quenching mechanisms and extinction coefficients cannot be ruled out.

The effect of urea on frequency response curves of W19F, as in the case of the total intensity plots, was opposite that obtained for W99F. Urea resulted in a shift to lower frequency of the profiles at all wavelengths, indicating a urea-induced increase in the fluorescence lifetime (Fig. 8A–C). Again, a number of analysis schemes were assayed. In unlinked analyses, a component with a value between 0.3 and 1.4 ns was apparent in all 27 data sets, with a value between 0.3 and 0.8 ns in 24 of 27 data sets. The fractional contribution of this component decreased significantly upon increasing the urea concentration. A second component between 1.9 and 3.6 ns in the unlinked analyses, and a longer component between 3.6 and 10.5 ns, both increased significantly in importance upon increasing the urea concentration. Not surprisingly, given the similarities of the unlinked fits, linking of lifetimes across both wavelength and urea concentration proved to be reasonable. The global χ^2 of the fit was 2.9, and all but one data set (2 M urea 380 nm, local $\chi^2 = 11$) were compatible with the linkage scheme. The DAS for urea unfolding of W19F recovered using this scheme are shown in Figure 6B. The three recovered lifetime components, 0.57, 2.4, and 5.0 ns, were similar to those recovered in the more complete wavelength study conducted previously on the native proteins (Royer, 1992). In that study, components at 0.53, 2.8, and 15 ns were observed, although the latter was not well resolved, with a 67% confidence limit for any value above 6 ns. The evolution of the DAS for W19F in the present study (Fig. 6B) reveals that all three components shift red with increasing urea concentration. The molecular fraction of the 0.57-ns component, alpha tau 3, decreases in the range of the main unfolding transition at all three wavelengths (Fig. 4B). This loss of the 0.53-ns component in favor of the longer lifetime is primarily responsible for the large increase in intensity seen in Figure 2B. The total intensity at 380 nm, for example, increases 2.4-fold over the range of 0–8 M urea, whereas the average lifetime (molecular fraction weighted) increases 2.5-fold over the same range, indicating that the change involves mainly the dynamic quenching mechanism, although the red shift in emission also contributes to steady-state intensity changes at that wavelength.

Discussion

Given the three-dimensional structure of the *trp* aporepressor protein (Zhang et al., 1987; see Kinemage 1) and

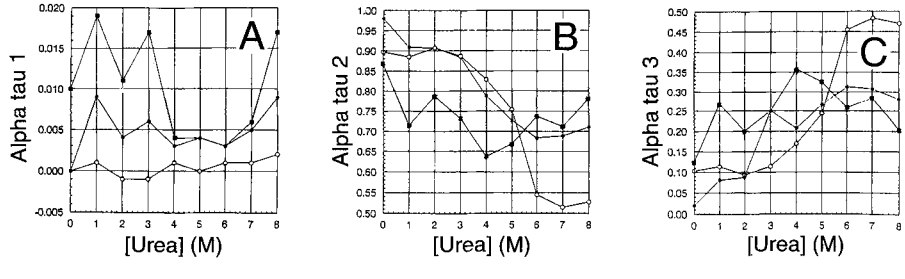

Fig. 7. Evolution of the pre-exponential factors, alpha tau (in population fraction, not fractional intensity), for the three components recovered from the fit of W99F. **A:** Alpha tau 1 (20 ns). **B:** Alpha tau 2 (4.3 ns). **C:** Alpha tau 3 (0.75 ns). Emission at 320 nm (○), 350 nm (●), and 380 nm (■).

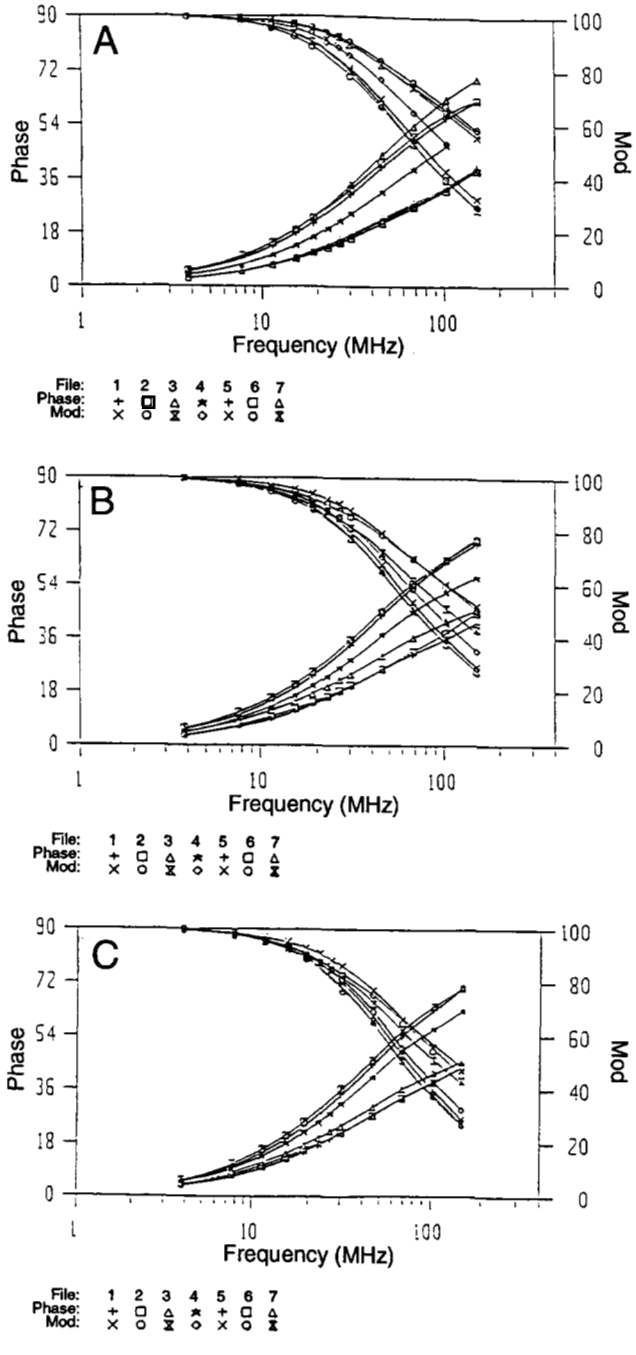

Fig. 8. Frequency response profiles of the intrinsic fluorescence of W19F at 0, 1, 2, 5, 6, 7, and 8 M urea. Mod and Phase indicate the modulation ratio and phase angle, respectively. Symbols numbered 1–6 correspond to the phase angles and modulation ratios for the six urea concentrations (0, 1, 2, 5, 6, 7, and 8 M). **A:** A 320-nm emission wavelength. **B:** A 350-nm emission wavelength. **C:** A 380-nm emission wavelength. Excitation was at 295 nm and protein concentration was 6.1 μM in dimer.

the equilibrium urea-unfolding profiles of its single tryptophan mutants, a physical interpretation of the observed fluorescence changes in the wild-type protein is possible. The loss in the fractional population of the 0.5-ns component implies that the large increase in fluorescence intensity upon unfolding arises from relief of the quenching of Trp 99. Examination of the three-dimensional structure (Zhang et al., 1987) reveals that Trp 99 is in van der Waals contact with the epsilon amide group of Asn 32 on the opposite subunit (Royer, 1992). Upon disruption of the dimer interface, this contact would be broken and quenching of the fluorescence of Trp 99 would be relieved. The red shift in emission results from exposure of the tryptophan to solvent.

Trp 19, which is buried at the subunit interface in the native structure and thus exhibits a very blue-shifted emission in this state, is highly red shifted upon unfolding. Presumably, this effect is also due to disruption of the subunit interface and exposure of the fluorophore to water. The fluorescence lifetime of Trp 19 exhibits a slight overall decrease compared to the main unfolding transition, perhaps due to a greater degree of flexibility, which could allow more efficient quenching by nearby groups such as His 16. Thus, changes in the fluorescence signal monitored upon unfolding of TR are consistent with disruption of the dimer interface and, presumably, appearance of the unfolded monomer.

Although interpretation of the changes observed in the main unfolding transition is relatively straightforward, explanations for the pre- and posttransition intensity (and lifetime) increases are less obvious. In the pretransition zone, residual oligomers dissociate to dimers with increasing urea (Fernando & Royer, 1992b). Although tryptophan emission exhibits no large changes upon oligomer dissociation (other than a decrease in fluorescence polarization), some of these subtle intensity changes may arise from oligomer dissociation. The continued effect of urea on both Trp 19 and Trp 99 at high urea concentrations (5–8 M) is due in part to the urea-induced increase in quantum yield of tryptophan. The urea-induced intensity change in the high urea concentration range is more pronounced for the TR mutants (23%) than for NATA (14%) within the range of 5–8 M urea. Grinvald and Steinberg (1976) report a 1-ns increase in the fluorescence lifetime of NATA in the range of 0–8 M urea; thus, the direct effect of urea on the intensity involves dynamic quenching mechanisms. However, because the direct effect of urea on NATA in the posttransition zone is significantly smaller than that on the intrinsic tryptophan fluorescence of the proteins, it may be that urea also affects the structure of the unfolded form of the proteins. Neri et al. (1992) have observed residual structure involving a tryptophan residue in the 434 repressor protein in 7 M urea.

In general, intrinsic tryptophan fluorescence properties of proteins change upon unfolding of the native conformation. The only change that can be predicted with confidence is that the emission spectrum will shift to red upon greater exposure to solvent. Changes in fluorescence intensity, however, are completely unpredictable (Kronman & Holmes, 1971). The local environments in native pro-

tein structures can result in either very large or very small quantum yields, leading to fluorescence lifetimes from less than 10 ps to near 10 ns (Beechem & Brand, 1985). Thus, unfolding of the structure could result in either an increase or a decrease in the fluorescence quantum yield. In addition to the variability of quantum yields in the native structure, similar variabilities are observed in the unfolded form (Kronman & Holmes, 1971). For example, the two tryptophan residues in unfolded TR exhibit lifetimes near 3–4 ns on average, slightly higher than that of NATA in water. In contrast, the single tryptophan in staphylococcal nuclease is highly quenched in the unfolded form (Eftink et al., 1989, 1991), with an average lifetime shorter than 1 ns (Eftink et al., 1989). The nonuniformity of tryptophan decay rates and quantum yields (Kronman & Holmes, 1971) in unfolded proteins indicates that residual interactions involving these fluorophores are a common phenomenon.

The results with TR underscore the importance of monitoring wavelength dependence of a variety of fluorescence properties of intrinsic tryptophan residues in protein-unfolding experiments. When the three-dimensional structure of the native protein is available, the information can provide a more detailed interpretation of structural changes that occur during unfolding. In this study, fluorescence changes at both tryptophan residues could be ascribed to disruption of the subunit interface of TR.

Despite perturbation of the stability of TR resulting from the single tryptophan to phenylalanine substitution, this approach has allowed us to use changes in fluorescence properties of the remaining tryptophan residue in each of these mutants to make a structural interpretation of changes in fluorescence observed upon unfolding of wild-type protein. As described in the accompanying paper (Mann et al., 1993), comparison of the fluorescence and circular dichroism equilibrium data demonstrates that unfolding of both mutants by urea involves an alteration in equilibrium behavior, indicating the presence of one or more stable intermediates.

Materials and methods

Site-directed mutagenesis

Full details of mutagenesis procedures are described in Mann et al. (1993). Briefly, the wild-type TR gene was removed from pJPR2 (Paluh & Yanofsky, 1986) and inserted into the replicative form of M13mp19 DNA to produce mp19-*trp*R. Uracil-containing single-stranded DNA was produced (Kunkel et al., 1987) and hybridized with the appropriate mutagenic oligonucleotide. Double-stranded DNA was used to transfect competent DH5αF′ cells (Hanahan, 1985), and the resulting viral plaques were used to prepare single-strand DNA for sequencing and identification of mutants (Sanger et al., 1980). The mutated *trp*R DNA was removed from the mp19-*trp*R construct and recloned into pJPR2 for protein expression.

Protein purification

Purification procedures used for TR mutant repressors were similar to those described for purification of wild-type TR (Paluh & Yanofsky, 1986; Chou et al., 1989). Protein purity was verified by the presence of a single band on Coomassie blue-stained sodium dodecyl sulfate-polyacrylamide gels (Schagger & von Jagow, 1987). Protein concentrations were determined by UV absorbance at 280 nm (Gill & von Hippel, 1989). Calculated extinction coefficients were 27,500 M^{-1} cm^{-1} for wild type, 16,400 M^{-1} cm^{-1} for W19F, and 16,400 M^{-1} cm^{-1} for W99F (Mann et al., 1993). DNA-binding assays were performed as described previously (Carey, 1988). DNA-binding affinities for the single tryptophan mutants were found to differ by less than 50% from wild-type TR (Mann et al., 1993).

Fluorescence measurements

Steady-state fluorescence emission spectra were performed on an ISS Koala automated spectral acquisition unit (ISS Inc., Champaign, Illinois), with excitation from a xenon arc lamp and the excitation monochromator set at 295 nm. Excitation and emission bandwidths were 8 nm. Time-resolved measurements were performed in the frequency domain using ISS frequency domain acquisition electronics. Excitation light at 295 nm was obtained by frequency doubling the output of a Coherent cavity-dumped 701 dye laser, which was excited with the 532 line of a Coherent frequency-doubled mode-locked ND-YAG Antares laser (Coherent Corporation, Palo Alto, California). The reference lifetime compound was *p*-terphenyl, with a lifetime of 1.0 ns in cyclohexane (Gratton et al., 1984). Phase and modulation data were collected until errors were less than 0.2 and 0.004° of phase and modulation units, respectively. Excitation was polarized at the magic angle. Solutions were less than 0.1 OD units at 295 nm, minimizing inner filter effects.

Buffers and reagents

All buffers were 10 mM potassium phosphate, 0.1 mM EDTA, pH 7.6. Ultrapure urea was purchased from ICN Biomedicals (Cleveland, Ohio). Solutions of proteins were pre-equilibrated with the urea-containing buffers for several hours. All changes in optical properties were complete before measurements were made.

Data analysis

Data were analyzed with the global analysis software developed by Beechem et al. (1991) (Globals Unlimited,

LFD, Urbana, Illinois). Generally, linking schemes involved sums of exponential decays in which lifetime values were linked across wavelengths or mutant protein data sets, whereas pre-exponential factors were allowed to vary.

Acknowledgments

This work was supported by the National Institute of General Medical Sciences, grant GM39969 (to C.A.R.), by National Institutes of Health postdoctoral fellowship award GM13571 (to C.J.M.), and by the National Institute of General Medical Sciences, grant GM23303 (to C.R.M.).

References

Axelson, P.H., Bajzer, Z., Prendergast, F.G., Cottam, P.F., & Ho, C. (1991). Resolution of the fluorescence intensity decays of the two tryptophan residues in glutamine-binding protein from *Escherichia coli* using single tryptophan mutants. *Biophys. J. 60*, 650-659.

Beechem, J.M. & Brand, L. (1985). Time-resolved fluorescence of proteins. *Annu. Rev. Biochem. 54*, 43-71.

Beechem, J.M., Gratton, E., Ameloot, M.A., Knutson, J.R., & Brand, L. (1991). Global analysis of fluorescence decay data: Second generation theory and programs. In *Fluorescence Spectroscopy. Principles and Techniques*, Vol. I (Lakowicz, J.R., Ed.), pp. 241-301. Plenum Press, New York.

Carey, J. (1988). Gel retardation at low pH resolves *trp* repressor-DNA complexes for quantitative study. *Proc. Natl. Acad. Sci. USA 85*, 975-979.

Chou, W.-Y., Bieber, C., & Matthews, K.S. (1989). Tryptophan and 8-anilino-1-naphthalenesulfonate compete for binding to *trp* repressor. *J. Biol. Chem. 264*, 18309-18313.

Eftink, M.R., Ghiron, C.A., Kautz, R.A., & Fox, R.O. (1989). Fluorescence lifetime studies with staphylococcal nuclease and its site-directed mutant. Test of the hypothesis that proline isomerization is the basis for nonexponential decays. *Biophys. J. 55*, 575-579.

Eftink, M.R., Gryczynski, I., Wiczk, W., Laczko, G., & Lakowicz, J.R. (1991). Effects of temperature on the fluorescence intensity and anisotropy decays of staphylococcal nuclease and the less stable nuclease-ConA-SG28 mutant. *Biochemistry 30*, 8945-8953.

Fernando, T. & Royer, C.A. (1992a). Role of protein-protein interactions in the regulation of transcription by *trp* repressor investigated by fluorescence spectroscopy. *Biochemistry 31*, 3429-3441.

Fernando, T. & Royer, C.A. (1992b). Unfolding of *trp* repressor studied using fluorescence spectroscopic techniques. *Biochemistry 31*, 6683-6691.

Gill, S.C. & von Hippel, P.H. (1989). Calculation of protein extinction coefficients from amino acid sequence data. *Anal. Biochem. 182*, 319-326.

Gittelman, M.S. & Matthews, C.R. (1990). Folding and stability of *trp* aporepressor from *Escherichia coli*. *Biochemistry 29*, 7011-7020.

Gratton, E., Limkemann, M., Lakowicz, J., Maliwal, B.P., Cherek, H., & Laczko, G. (1984). Resolution of mixtures of fluorophores using variable-frequency phase and modulation data. *Biophys. J. 46*, 479-486.

Grinvald, A. & Steinberg, I.Z. (1976). The fluorescence decay of tryptophan residues in native and denatured proteins. *Biochim. Biophys. Acta 427*, 663-678.

Hanahan, D. (1985). Techniques for transformation of *Escherichia coli*. In *DNA Cloning: A Practical Approach*, Vol. 1 (Glover, D.M., Ed.), pp. 109-135. Oxford University Press, Oxford, UK.

Harris, D.L. & Hudson, B.S. (1990). Photophysics of tryptophan in bacteriophage in T4 lysozymes. *Biochemistry 29*, 5276-5285.

Kronman, M.J. & Holmes, L.G. (1971). The fluorescence of native, denatured and reduced-denatured proteins. Photochem. Photobiol. 14, 113-134.

Kunkel, T.A., Roberts, J.D., & Zakour, R.A. (1987). Rapid and efficient site-specific mutagenesis without phenotypic selection. *Methods Enzymol. 154*, 367-383.

Lane, A.N. & Jardetsky, O. (1987). Unfolding of the *trp* repressor from *Escherichia coli* monitored by fluorescence, circular dichroism and nuclear magnetic resonance. *Eur. J. Biochem. 164*, 389-396.

Mann, C.J., Royer, C.A., & Matthews, C.R. (1993). Tryptophan replacements in the *trp* aporepressor from *Escherichia coli*: Probing the equilibrium and kinetic folding models. *Protein Sci. 2*, 1853-1861.

Neri, D., Billeter, M., Wider, G., & Wüthrich, K. (1992). NMR determination of residual structure in a urea-denatured protein, the 434-repressor. *Science 257*, 1559-1563.

Pace, C.N. (1986). Determination and analysis of urea and guanidine hydrochloride denaturation curves. *Methods Enzymol. 131*, 266-280.

Paluh, J.L. & Yanofsky, C. (1986). High level production and rapid purification of the *E. coli trp* repressor. *Nucleic Acids Res. 14*, 7851-7860.

Royer, C.A. (1992). Investigation of the structural determinants of the intrinsic fluorescence emission of the *trp* repressor using single tryptophan mutants. *Biophys. J. 63*, 741-750.

Royer, C.A., Gardner, J.A., Beechem, J.M., Brochon, J.-C., & Matthews, K.S. (1990). Resolution of the fluorescence decay of the two tryptophan residues of *lac* repressor using single tryptophan mutants. *Biophys. J. 58*, 363-377.

Sanger, F., Coulson, A.R., Barrell, B.G., Smith, A.J., & Roe, B.A. (1980). Cloning in single-stranded bacteriophage as an aid to rapid DNA sequencing. *J. Mol. Biol. 143*, 161-178.

Schagger, H. & von Jagow, G. (1987). Tricine-sodium dodecyl sulfate-polyacrylamide gel electrophoresis for the separation of proteins in the range from 1 to 100 kDa. *Anal. Biochem. 166*, 368-379.

Tanford, C. (1970). Protein denaturant: Part C. Theoretical models for the mechanism of denaturation. *Adv. Protein Chem. 24*, 1-95.

Zhang, R.-G., Joachimiak, A., Lawson, C.L., Schevitz, R.W., Otwinowski, Z., & Sigler, P.B. (1987). The crystal structure of *trp* aporepressor at 1.8 Å shows how binding tryptophan enhances DNA affinity. *Nature 327*, 591-597.